AMERICAN ACADEMY OF OPHTHALMOLOGY®

Disease Activity and Therapeutic Response to Pegcetacoplan for Geographic Atrophy Identified by Deep Learning-Based Analysis of OCT

Ursula Schmidt-Erfurth, MD,[1] *Julia Mai, MD,*[1] *Gregor S. Reiter, MD, PhD,*[1] *Sophie Riedl, MD, PhD,*[1] *Wolf-Dieter Vogl, PhD,*[2] *Amir Sadeghipour, PhD,*[2] *Alex McKeown, PhD,*[3] *Emma Foos, BA, MPH,*[3] *Lukas Scheibler, PhD,*[3] *Hrvoje Bogunovic, PhD*[1]

Purpose: To quantify morphological changes of the photoreceptors (PRs) and retinal pigment epithelium (RPE) layers under pegcetacoplan therapy in geographic atrophy (GA) using deep learning–based analysis of OCT images.

Design: Post hoc longitudinal image analysis.

Participants: Patients with GA due to age-related macular degeneration from 2 prospective randomized phase III clinical trials (OAKS and DERBY).

Methods: Deep learning–based segmentation of RPE loss and PR degeneration, defined as loss of the ellipsoid zone (EZ) layer on OCT, over 24 months.

Main Outcome Measures: Change in the mean area of RPE loss and EZ loss over time in the pooled sham arms and the pegcetacoplan monthly (PM)/pegcetacoplan every other month (PEOM) treatment arms.

Results: A total of 897 eyes of 897 patients were included. There was a therapeutic reduction of RPE loss growth by 22% and 20% in OAKS and 27% and 21% in DERBY for PM and PEOM compared with sham, respectively, at 24 months. The reduction on the EZ level was significantly higher with 53% and 46% in OAKS and 47% and 46% in DERBY for PM and PEOM compared with sham at 24 months. The baseline EZ-RPE difference had an impact on disease activity and therapeutic response. The therapeutic benefit for RPE loss increased with larger EZ-RPE difference quartiles from 21.9%, 23.1%, and 23.9% to 33.6% for PM versus sham (all $P < 0.01$) and from 13.6% ($P = 0.11$), 23.8%, and 23.8% to 20.0% for PEOM versus sham ($P < 0.01$) in quartiles 1, 2, 3, and 4, respectively, at 24 months. The therapeutic reduction of EZ loss increased from 14.8% ($P = 0.09$), 33.3%, and 46.6% to 77.8% ($P < 0.0001$) between PM and sham and from 15.9% ($P = 0.08$), 33.8%, and 52.0% to 64.9% ($P < 0.0001$) between PEOM and sham for quartiles 1 to 4 at 24 months.

Conclusions: Deep learning-based OCT analysis objectively identifies and quantifies PR and RPE degeneration in GA. Reductions in further EZ loss on OCT are even higher than the effect on RPE loss in phase 3 trials of pegcetacoplan treatment. The EZ-RPE difference has a strong impact on disease progression and therapeutic response. Identification of patients with higher EZ-RPE loss difference may become an important criterion for the management of GA secondary to AMD.

Financial Disclosure(s): Proprietary or commercial disclosure may be found after the references. *Ophthalmology 2025;132:181-193 © 2024 by the American Academy of Ophthalmology. This is an open access article under the CC BY-NC-ND license (http://creativecommons.org/licenses/by-nc-nd/4.0/).*

Supplemental material available at www.aaojournal.org.

One of the major unresolved challenges in ophthalmology and a cause of severe visual loss globally, geographic atrophy (GA) due to age-related macular degeneration (AMD) has been untreatable until recently. Positive outcomes of phase III clinical trials have led to hopes for widespread availability of GA treatment.[1,2] Accordingly, regulatory approval by the Food and Drug Administration (FDA) was granted, and the substances used for intravitreal therapy have become accessible for clinical use in the United States and are under review in Europe.

This marks a major advance after years of research into the role of the complement system, particularly the inhibition of complement factor 3 (C3), in the pathogenesis of GA. Complement-induced biological interactions at the macular location of GA include effects on neurosensory components such as glial cells and photoreceptors (PRs) as well as the retinal pigment epithelium (RPE) and the supporting choriocapillary layer.[1–3] All these compartments are known locations of disease activity in AMD,

https://doi.org/10.1016/j.ophtha.2024.08.017
ISSN 0161-6420/24

particularly in GA, and may likely contribute to disease activity and progression in an interactive multifactorial manner.[4]

In the absence of therapy, GA has been largely underdiagnosed because of a lack of referrals to a retina service and unsatisfactory assessment with standardized imaging techniques.[5] With regulatory approval of 2 therapies for GA in the United States in 2023, this deficiency is changing drastically, and GA now has to be rapidly referred into an adequate standard of care. Accordingly, physicians need to develop a robust risk/benefit assessment and reimbursement strategies are required.[6] Previously, fundus autofluorescence (FAF) was introduced because of the ability to visualize the presence of fluorescent metabolites in healthy RPE cells and nonfluorescence in atrophic areas.[7] Indeed, FAF-based determination of RPE loss in observational studies demonstrated progressive lesion expansion in GA and was used to follow the average speed of growth with a large variability in GA progression seen.[8] However, OCT is the preferred method to diagnose and monitor GA in the clinical routine of AMD and represents the critical features of GA activity and variability at the neurosensory level.[9]

With the rapid advances in OCT technology, spectral-domain OCT has become the state-of-the-art diagnostic tool in the management of AMD.[10] The high-resolution properties of a current standard OCT scan allow an unprecedented insight into the neurosensory morphology of the retina, the RPE layer, and the choroidal vasculature.[11] The focus of diagnostic imaging in AMD, and OCT in general as the most frequent diagnostic measure in all medicine, has from its beginning been tightly associated with therapeutic interventions. It combines high precision and practicality for optimal image acquisition, which is needed for an efficient evaluation of GA because the technology is able to capture 2 major anatomic components, namely, the PR and the RPE layers on a pixel base.[12]

Another technological advance that has recently spread through OCT image analyses with much emphasis is artificial intelligence (AI) for OCT-based image analysis. Artificial intelligence techniques such as deep learning have provided proof-of-principle to visualize integrity and pathology at the level of the PR and RPE layer in a quantitative manner.[13,14] The PR layer is the morphological correlate of retinal function and therefore of major interest for the clinical evaluation of any GA therapy.[15,16] It is represented on an OCT scan by the ellipsoid zone (EZ) with the mitochondrial center and the outer PR segments. Automated and objective diagnostic tools and the related biomarkers, such as the RPE and EZ layer, yet have to undergo rigorous scrutiny to qualify for consideration as adequate outcome parameters in clinical trials and even more so regarding their promise in clinical practice. Photoreceptor loss is defined in our article as EZ layer loss on the OCT image. This is in line with the FDA's approval of EZ loss as a primary outcome marker in another degenerative macular disease, macular telangiectasis,[17,18] and the recent FDA acknowledgment of EZ loss for clinical GA trials.[19]

The study population and imaging data of the phase 3 clinical trials of OAKS and DERBY represent the largest data set in a successful GA therapy program to date and offer a unique perspective for evaluating the potential of state-of-the-art AI-based OCT analysis. The deep-learning tools that we are applying have previously undergone extensive validation and achieve a performance that does not require manual correction. It has been shown that the performance of the algorithms lies within the intergrader agreement of expert graders.[20,21] The aim of the present analyses is to examine on the critical PR/RPE level whether clinical mechanisms of GA disease can be elucidated beyond current knowledge, which OCT-related parameters may objectively reflect disease activity, and which type of therapeutic response can be expected and objectively monitored.

Methods

Inclusion and Treatment Arms

This investigation is an analysis of OCT data from 2 identical prospective 24-month, multicenter, randomized, double-masked, sham-controlled, phase 3 trials (OAKS, NCT03525613; DERBY, NCT03525600). Written informed consent was obtained from all patients before any study-related procedure, and both studies adhered to the tenets of the Declaration of Helsinki. This post hoc analysis was approved by the Ethics Committee of the Medical University of Vienna.

For both OAKS and DERBY, patients were randomized 2:2:1:1 to receive pegcetacoplan 15 mg/0.1 mL monthly (PM), pegcetacoplan 15 mg/0.1 mL every other month (PEOM), sham monthly, or sham every other month over a 24-month follow-up period. In the first year, all patients were scheduled for monthly study visits, whereas in the second year, patients in any "every other month" treatment arm were scheduled for bimonthly study visits.

Inclusion criteria were $>$ 60 years of age, best-corrected visual acuity (BCVA) of $\geq$ 24 letters on the ETDRS chart (Snellen equivalent 20/320, 0.06 decimal), and a diagnosis of GA secondary to AMD. Only eyes with a GA area of 2.5 to 17.5 mm^2 were eligible for inclusion. If GA configuration was multifocal, at least 1 lesion had to be larger than 1.25 mm^2. All GA characteristics for inclusion were measured by FAF, and a perilesional pattern of hyperautofluorescence was mandatory. If both eyes were eligible, the eye with the worse BCVA was designated as the study eye. Eyes with active macular neovascularization (MNV), defined as exudative MNV showing retinal fluid, were excluded as potential study eyes. Nonexudative MNV has not been excluded in this study. Macular neovascularization in the fellow eye was not an exclusion criterion. Both subfoveal and nonsubfoveal GA lesions were eligible for inclusion. Full details of the inclusion/exclusion criteria have been published previously.[22]

OCT Imaging

Patients included in this analysis underwent OCT imaging with the Spectralis HRA+OCT (Heidelberg Engineering). The acquisition included a macula-centered volumetric raster scan, covering a 20° $\times$ 20° field of view (FOV), consisting of 49 B-scans with 120 μm spacing, with each containing 512 A-scans, and with an ART (frame averaging) setting of 16. The scans were acquired with a follow-up function available on the Spectralis device to keep the anatomic consistency of the FOV over the visits. Longitudinal

imaging data up to month 24 were used with a consistent and continuous bimonthly imaging pattern to match the "every other month" imaging protocol. All OCT volumes were quantified using validated and precise AI algorithms. Participants who underwent OCT imaging with devices other than Spectralis were not included in this analysis, because AI-based algorithms must be trained and validated in a device-specific manner to reach high performance. OCT image quality per se was not evaluated in addition because the quality was high because the images were acquired as part of a clinical trial according to a tight protocol and following certification of the operators controlled by an independent reading center.

Artificial Intelligence Methods Used for RPE Loss and EZ Layer Loss

Artificial Intelligence–Based RPE Loss Measurements. The volumetric OCT scan was provided as input to a deep learning algorithm trained for the task of RPE loss segmentation, where all the A-scans found to contain absence of RPE cells were automatically identified. The algorithm is based on a specialized convolutional neural network designed to delineate 2-dimensional en face GA areas, as described previously.[23] The design enables parallel processing of the A-scans, taking a few seconds to process an entire OCT volume in a context-based approach. It was trained and previously validated on multiple datasets, most notably on the FILLY clinical trial, the phase II predecessor to DERBY and OAKS, showing that it can segment GA areas on OCT coming from clinical trials with high accuracy and within inter-grader variability.[21] Finally, an en face RPE loss map was derived for each volumetric OCT scan, and the area of RPE loss was used for subsequent analyses.

Artificial Intelligence–Based Ellipsoid Zone Layer Loss Measurements. The PR layer, defined as EZ layer on OCT, was delineated on every B-scan using a composite convolutional neural network for pixel-level segmentation specifically trained to segment a specific retinal layer defined to lie between the upper boundary of EZ and the upper boundary of RPE (the outer boundary of the interdigitation zone), as described previously.[24] The resulting EZ layer thickness in patients with GA originating from the FILLY trial was validated previously and shown to have a mean precision within the resolution of the OCT scanner.[20] To detect the A-scans exhibiting EZ loss, an EZ thickness of $\leq$ 4 μm was considered. Finally, an en face EZ integrity loss map was derived for each volumetric OCT scan.

OCT Scan–Derived Measurements. The 2 segmented en face maps were brought in direct correspondence, and the areas of RPE loss were automatically designated to contain EZ loss as well. An ETDRS grid was then placed at the center of the OCT scan, and the RPE loss and EZ integrity loss areas within the 20° × 20° FOV were calculated and expressed in mm^2.

End Points

In both studies, the end points assessed were the change from baseline in EZ layer loss area and RPE loss area in the total FOV.

Statistical Analysis

Patients in the sham monthly and sham every-other-month groups were pooled into a single control group for all analyses (henceforth referred to as "sham"). All efficacy analyses were done using the modified in intention-to-treat population, which was defined as all patients who received 1 or more injections of pegcetacoplan or sham and had a baseline and at least 1 postbaseline value of GA lesion area measured by FAF in the study eye and used for the primary efficacy analyses in the DERBY and OAKS studies, with at least 1 quantifiable EZ integrity loss area or RPE loss area measurement from a Spectralis HRA+OCT image.

To assess the therapeutic effect on EZ and RPE layer maintenance, a mixed-effect model for repeated measures was used to measure the least-squares mean change from baseline to month 24 for each end point. The variables in the model included treatment (PM, PEOM, sham), stratification factors (history or presence of fellow eye MNV at baseline and baseline GA lesion area (< 7.5 mm^2 or ≥ 7.5 mm^2), baseline loss area of end point assessed (RPE or EZ layer), time as a factor, time by treatment interaction term, and baseline loss area by time interaction term. An unstructured covariance matrix was used to model the within-patient errors.

To assess the impact of the baseline EZ-RPE loss difference on future disease progression as well as differences in therapeutic response, the 2 studies were pooled, and patients were split into quartiles of baseline EZ-RPE loss difference. Descriptive statistics were used to assess the progression rates for RPE loss on OCT as well as GA lesion growth on FAF over time in the sham patients. Therapeutic response was assessed within each quartile using the same analysis as described above for all patients with the addition of an indicator variable for study as a covariate. Additional analyses were done to evaluate the progression rate based on FAF measurements as well as therapeutic response between OCT-based EZ-RPE difference quartiles performing a square root transformation.[25]

This is a post hoc analysis of imaging data from the OAKS and DERBY studies, P values are not controlled for multiplicity (nominal).

Results

A total of 897 eyes from 897 patients (74.1% of entire trial) were included in this analysis that were imaged with a Spectralis OCT from both trials together. Baseline characteristics were well balanced between the groups regarding age, sex, and ethnicity (Table 1). Mean lesion size in mm^2 on FAF was 8.2, two-thirds of lesions were subfoveal, approximately 80% were bilateral GA, and 20% of study eyes demonstrated MNV in the fellow eye. In the PM, PEOM, and sham arms, 276, 281, and 293 eyes, respectively, completed the 12-month follow-up and 237, 255, and 265, respectively, were analyzed at 24 months. The flowchart of the study population is shown in Figure S1 (available at www.aaojournal.org).

Artificial Intelligence–Based Therapeutic Effect on EZ and RPE Maintenance on OCT

Treatment with pegcetacoplan reduced RPE loss growth versus sham, consistent with the lesion seen clinically on FAF. In OAKS, the reduction in RPE loss growth between PM and sham was 22% ($P = 0.0002$) and between PEOM and sham was 20% ($P = 0.0002$) at 24 months. In DERBY, the reduction between PM and sham was 27% ($P < 0.0001$) and between PEOM and sham was 21% ($P = 0.0005$) over 24 months of follow-up. This difference became manifest from the beginning of the study. The therapeutic effect on absolute values of RPE loss growth increased over time (Fig 1). Of note, the reduction in the growth of the mean area demonstrating EZ loss over time was substantially more pronounced, reaching a difference between PM and sham of 53% ($P < 0.0001$) and between PEOM and sham of 46% ($P < 0.0001$) in OAKS at 24 months. In DERBY,

Table 1. Patient Demographics and Disease Characteristics of the Study Population

Variable	PM	PEOM	Sham
Age, mean (yrs)	78.2	78.4	78.1
Female, n (%)	176 (60.9)	169 (57.3)	196 (63.8)
White, n (%)	264 (91.3)	270 (91.5)	285 (92.8)
Study eye GA lesion size (FAF), mm^2	8.3	8.3	8.1
Study eye GA lesion size (FAF), square root (mm)	2.8	2.8	2.8
Study eye GA lesion location (FAF), n (%)			
Subfoveal involvement, n (%)	178 (61.6)	181 (61.4)	205 (66.8)
Without subfoveal involvement, n (%)	111 (38.4)	114 (38.6)	102 (33.2)
Study eye laterality			
Bilateral GA, n (%)	240 (83.0)	240 (81.4)	240 (78.2)
Study eye GA only, n (%)	49 (17.0)	55 (18.6)	67 (21.8)
Fellow eye advanced AMD status			
GA only, n (%)	209 (72.3)	215 (72.9)	210 (68.4)
Any MNV, n (%)	58 (20.1)	56 (19.0)	62 (20.2)
GA with MNV, n (%)	31 (10.7)	25 (8.5)	30 (9.8)
MNV only, n (%)	27 (9.3)	31 (10.5)	32 (10.4)
Neither GA nor MNV, n (%)	22 (7.6)	24 (8.1)	35 (11.4)

FAF = fundus autofluorescence; GA = geographic atrophy; MNV = macular neovascularization; PEOM = pegcetacoplan every other month; PM = pegcetacoplan monthly.

the reduction of EZ loss between PM and sham was 47% ($P < 0.0001$) and between PEOM and sham was 46% ($P < 0.0001$) at 24 months. The progression rate was lower for both pegcetacoplan treatment groups than for the sham pooled group starting at initiation of treatment.

Figure 2 visualizes the progression of an exemplary GA lesion for both layers, RPE and EZ, over time in the untreated fellow eye and the treated study eye (PM arm) of the same patient. The video representation captures the biologic dynamics of GA progression in an exemplary manner, shown in Video 1 (study eye) and Video 2 (fellow eye) (available at www.aaojournal.org): PR thinning due to EZ loss proceeds as the primary event and consistently precedes and exceeds RPE loss that follows the PR attenuation zone. At baseline, the RPE defects are located within the larger area of EZ loss in both eyes (Fig 2A, C). At the end of follow-up, in the treated eye enhanced maintenance of EZ integrity leads to a markedly smaller total lesion, particularly regarding the RPE loss defined clinically as GA lesion (Fig 2D). The fellow eye

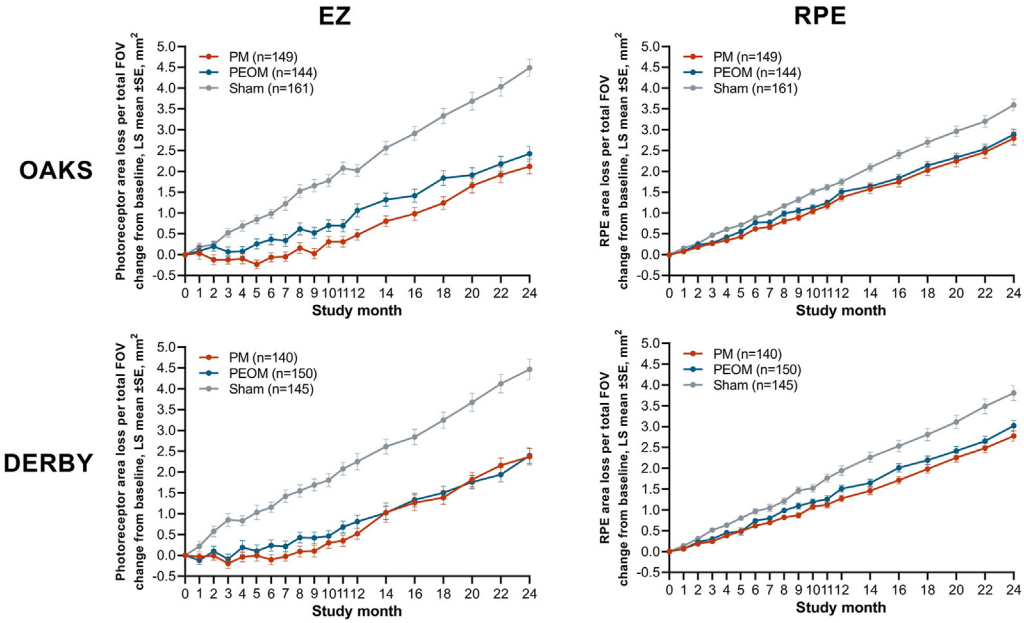

Figure 1. Artificial intelligence (AI)-based measurement of treatment effect of pegcetacoplan on ellipsoid zone (EZ) loss (left) and retinal pigment epithelium (RPE) loss (right) on OCT between sham and treatment groups in OAKS (upper row) and DERBY (lower row). FOV = field of view; LS = least square; PEOM = pegcetacoplan every other month; PM = pegetacoplan monthly; SE = standard error.

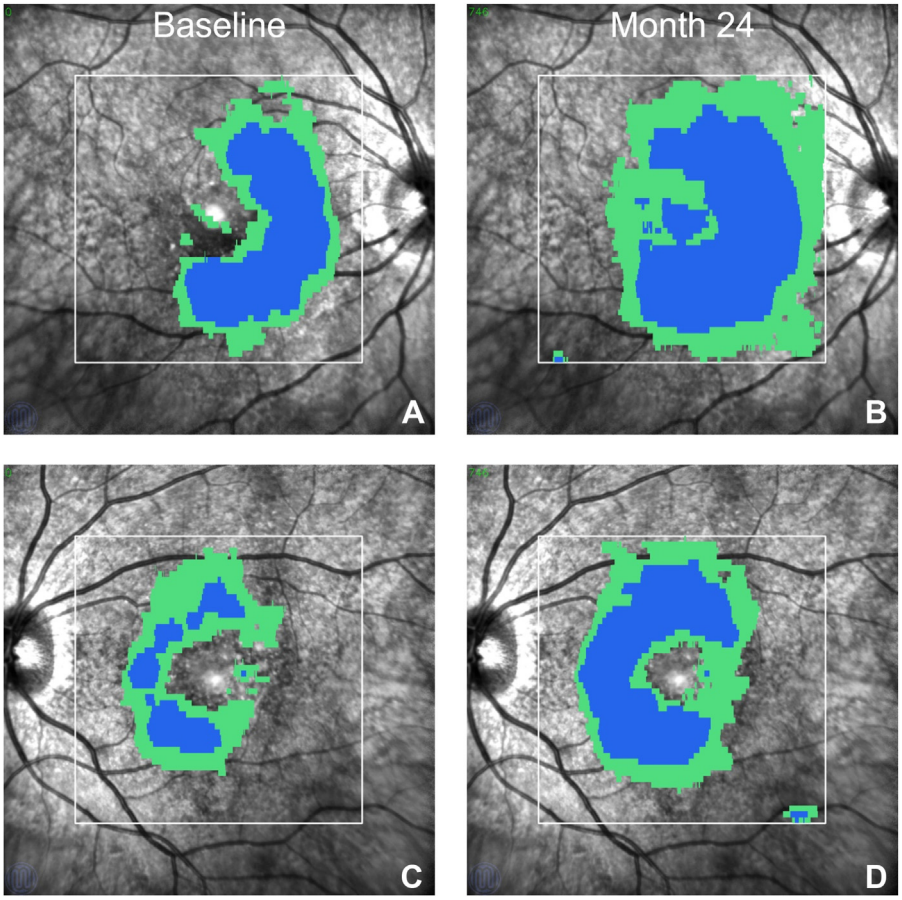

Figure 2. OCT-based evaluation of therapeutic efficacy. Comparison of retinal pigment epithelium (RPE) (blue) and ellipsoid zone (EZ) loss (green) growth in fellow eye (upper row) and study eye (lower row) in the PM arm. Both eyes show a high EZ-RPE loss difference at baseline **(A, C)**. The fellow eye shows an extensive growth at month 24 **(B)**, whereas the study eye shows reduced growth and protection of the fovea at month 24 (D).

shows an extensive growth over 24 months, including foveal involvement of the atrophic process (Fig 2B).

Impact of EZ-RPE Loss Difference on Disease Activity

When the lesions were split into quartiles of respective baseline EZ-RPE difference throughout the pooled sham arms of OAKS and DERBY, the impact of the EZ-RPE difference became manifest in a systematic manner (Fig 3). The quartiles based on EZ-RPE difference at baseline were as follows: quartile 1 (< 1.31 mm^2); quartile 2 (≥ 1.31) and < 2.82 mm^2); quartile 3 (≥ 2.82 and < 5.97 mm^2); and quartile 4 (≥ 5.97 mm^2). Geographic atrophy lesion growth (i.e., RPE loss growth) was strongly dependent on the baseline EZ-RPE difference, with the smallest quartile expanding least and progressively greater baseline EZ-RPE quartiles progressing faster (Figure 3). In lesions with a small difference (i.e., a low EZ-RPE quartile), the expansion of the individual lesions over time was markedly slower than the OCT-based RPE loss and FAF-based GA lesion growth in eyes with a large difference at baseline (Tables S2–S4, available at www.aaojournal.org). The baseline EZ-RPE relationship assessed on OCT is also transferrable to FAF image grading (Fig S2, available at www.aaojournal.org). The quartiles showed similar separation between Q1 and Q4 to the trends seen in Figure 3, including square root–transformed assessment of GA lesion growth on FAF. The videos in the Supplementary Material (available at www.aaojournal.org) impressively reveal this pathognomonic growth pattern (Video 3 low quartile, Video 4 high quartile): The GA lesion in Figure 4A started with a small EZ-RPE difference at first presentation and demonstrated only minimal growth over time (Fig 4B). In contrast, the lesion shown in Figure 4C demonstrated a large difference of the EZ loss area with small islands of RPE loss at baseline but enlarged rapidly with the RPE loss progressively filling into the preceding area of EZ loss (Fig 4D).

Impact of EZ-RPE Difference on Therapeutic Response

The same quartiles for baseline EZ-RPE differences were used to explore the effect on the therapeutic response at the level of both the EZ and RPE layer for both studies pooled. In the quartile with the lowest difference at baseline, the therapeutic effect on the RPE lesion was less pronounced

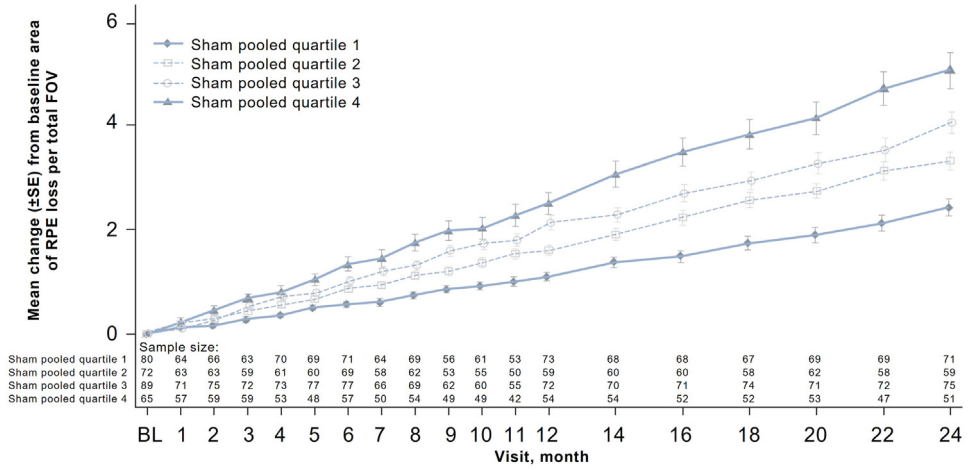

Figure 3. Disease activity by baseline ellipsoid zone (EZ)-retinal pigment epithelium (RPE) loss difference quartiles in sham patients pooled from OAKS and DERBY. Patients in the lowest quartile 1 show a slower progression, whereas patients in quartile 4 show a faster progression for RPE loss growth over 24 months. FOV = field of view; SE = standard error.

but increased proportionally with higher quartiles in the PM treatment group and was greater in quartile 4 (Fig 5). The reduction in RPE lesion growth at 24 months between sham and PM and PEOM was 21.9% ($P < 0.01$) and 13.6% ($P = 0.11$) in quartile 1; 23.1% ($P < 0.01$) and 23.8% ($P < 0.01$) in quartile 2; 23.9% ($P < 0.01$) and 23.8% ($P < 0.01$) in quartile 3; and 33.6% ($P < 0.0001$) and 20.0% ($P < 0.01$) in quartile 4, respectively (Fig 5). The same dependence of the treatment effect on EZ-RPE difference quartiles becomes manifest when evaluating GA lesion growth on FAF for both untransformed (Fig S3, available at www.aaojournal.org) and square root−transformed (Fig S4, available at www.aaojournal.org) GA growth assessment.

Regarding the effect of treatment on maintenance of EZ integrity, the therapeutic response dependent on the baseline EZ-RPE difference was more pronounced (Fig 6). Minimal difference between the sham and treatment arms was seen in the lowest quartile 1 with a steady increase in benefit over

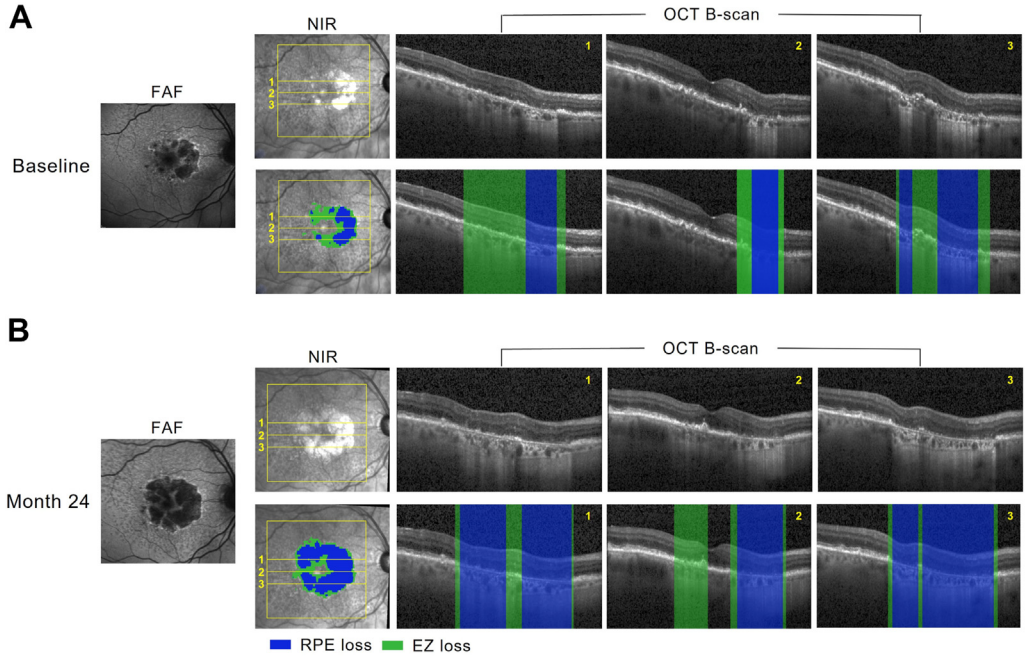

Figure 4. OCT-based evaluation of disease activity. The disease activity in geographic atrophy (GA) lesions is dependent on the ellipsoid zone (EZ)-retinal pigment epithelium (RPE) loss difference as shown in this example (blue = RPE loss, green = EZ loss). The example shows a GA lesion with a high EZ-RPE loss difference at baseline. The central B-scan as well as 1 B-scan above and 1 B-scan below are shown with and without segmentation for baseline (upper row) and month 24 (lower row), highlighting the progression of RPE loss growth in previously segmented EZ loss areas.

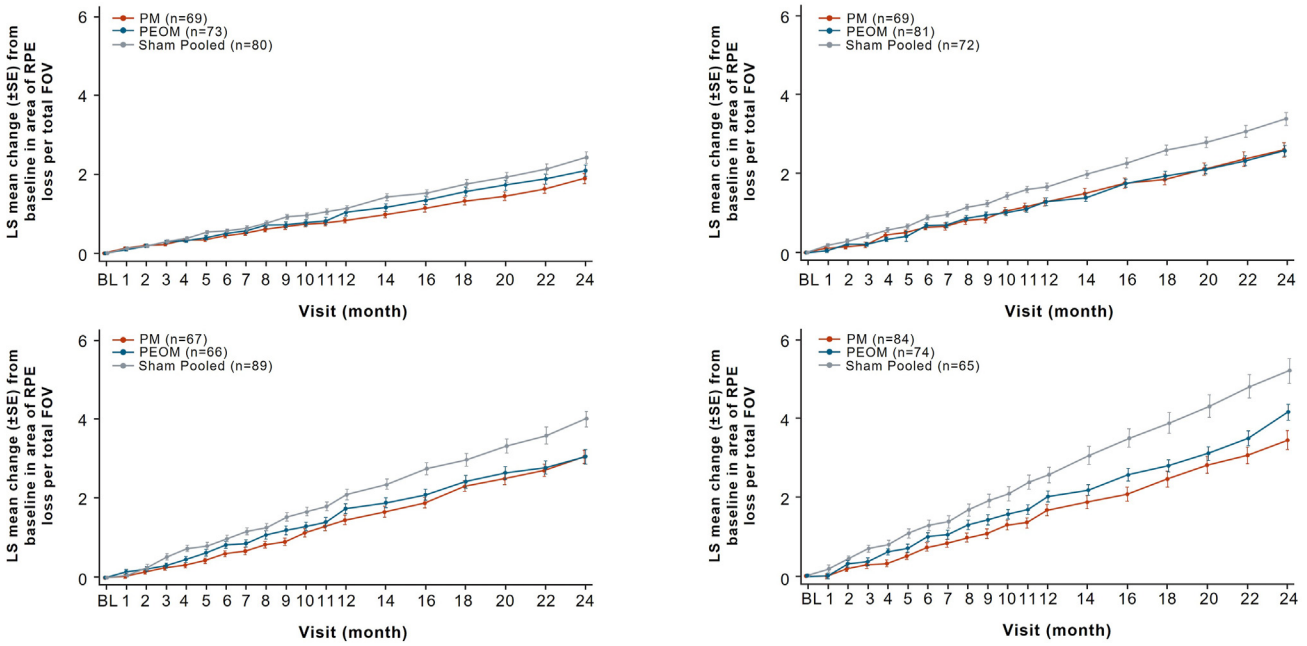

Figure 5. Difference of treatment effect for retinal pigment epithelium (RPE) loss growth between ellipsoid zone (EZ)-RPE loss difference quartiles. The treatment effect between pegcetacoplan monthly (PM)/pegcetacoplan every other month (PEOM) and sham increases from quartile 1 (upper left) over quartile 2 (upper right) and quartile 3 (lower left) and is most pronounced in quartile 4 (lower right). FOV = field of view; LS = least square; SE = standard error.

quartiles 2 and 3 and a most prominent improvement by therapeutic intervention in quartile 4. The reduction in EZ loss growth between sham and PM/PEOM in quartile 1 was 14.8% ($P = 0.09$) and 15.9% ($P = 0.08$), increasing to 33.3% ($P < 0.0001$) and 33.8% ($P < 0.0001$) in quartile 2 and further to 46.6% ($P < 0.0001$) and 52.0% ($P < 0.0001$) in quartile 3. The treatment benefit was largest in the quartile with the highest baseline EZ-RPE difference with a reduction of growth by 77.8% ($P < 0.0001$) and 64.9% ($P < 0.0001$). Statistical testing of the treatment effect between the quartiles revealed no nominally significant difference in untransformed and square root–transformed GA growth on FAF and RPE loss on OCT (Tables S5, S6, S8, and S9, available at www.aaojournal.org). An effect was observed for untransformed and square root–transformed OCT-based EZ loss between Q1 versus Q3, Q1 versus Q4, Q2 versus Q4, for PM and PEOM and for Q3 versus Q4 in the PM group and Q2 versus Q3 in the PEOM group (Tables S7 and S10, available at www.aaojournal.org).

Figure 7A and B show an overview of the quartiles of lowest and highest EZ-RPE difference in their change from baseline over 24 months for the pooled arms. With increasing quartiles, the difference in change in RPE loss becomes more pronounced (Fig 7A). The impact of the baseline EZ-RPE difference is most pronounced regarding the gain in therapeutic maintenance compared with the untreated progression of EZ loss in the sham arms (Fig 7B).

Discussion

In these analyses, we have applied 2 complementary and previously validated deep learning–based algorithms for GA evaluation to the largest phase 3 imaging set available from a successful therapeutic trial program. The unique combination allowed us to contribute in 3 clinically relevant ways to the state-of-the-art in the management of GA: identify pathognomonic patterns of GA progression, reveal mechanisms of complement inhibition as a therapeutic strategy, and provide prognostic features for disease activity and therapeutic response. All of those insights are novel and became accessible by the introduction of OCT-based, high-resolution segmentation identifying and quantifying subclinical biomarkers relevant in the process of GA disease. Most important, the described tools will be widely usable and practical after regulatory approval in a changing clinical routine that is about to arrive in a substantial dimension in retina practices worldwide.

First, a detailed and time-resolved visualization of the path of GA lesion progression could be derived from the sham groups of OAKS and DERBY. The relentless expansion of GA lesions in the affected macula of elderly individuals is well known. However, the individual variability of anatomic and functional progression is extremely high. Introducing deep learning–based segmentation of well-defined morphological features for PR detection and objective markers of PR degeneration such as EZ layer loss on OCT in GA enables a comprehensive visualization of pathognomonic patterns of lesion growth in GA over time. Correlation of the growth dynamics of the GA lesion in its 2 major components, PR and RPE, unveils the sequence of events with EZ loss preceding consecutive RPE loss in time and location. The size of the dataset in OAKS and DERBY with more than these 897 participants with available images for the present analysis allows us to translate this hypothesis to confirmatory evidence.

Second, our results shed innovative light on therapeutic mechanisms in GA, particularly complement inhibition as a

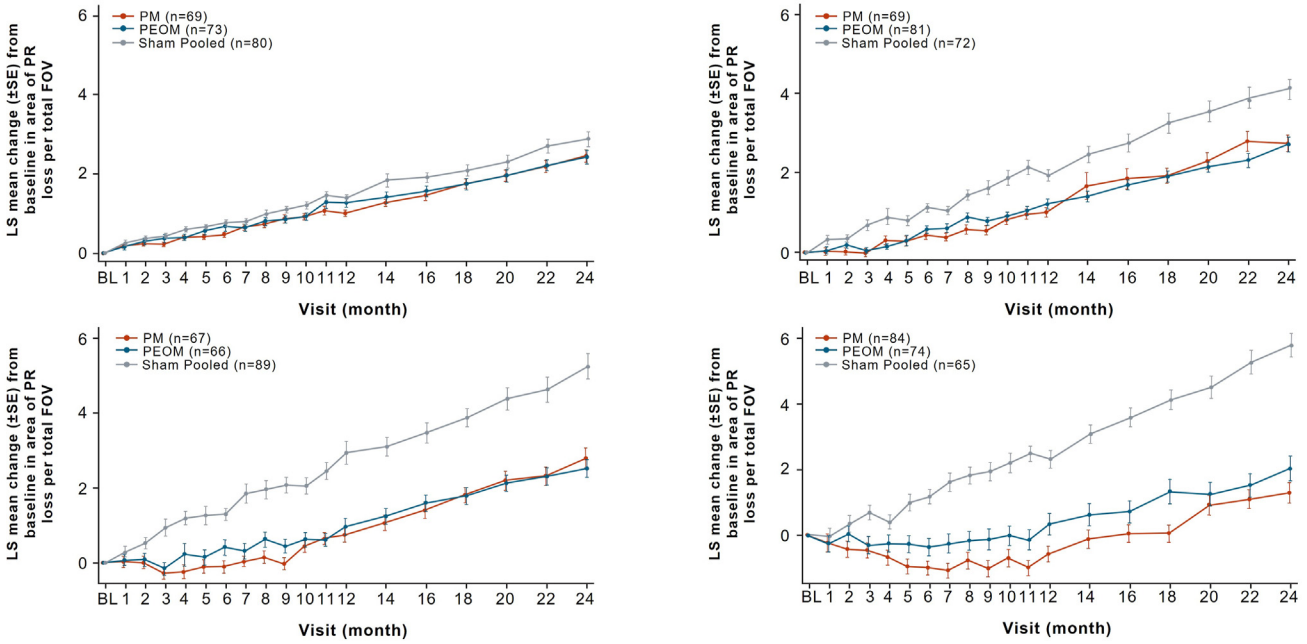

Figure 6. Difference of treatment effect for ellipsoid zone (EZ) loss growth between EZ-retinal pigment epithelium (RPE) loss difference quartiles. The treatment effect between pegcetacoplan monthly (PM)/pegcetacoplan every other month (PEOM) and sham increases from quartile 1 (upper left) over quartile 2 (upper right) and quartile 3 (lower left) and is most pronounced in quartile 4 (lower right). FOV = field of view; LS = least square; SE = standard error.

promising strategy. Complement as a therapeutic target received significant attention throughout recent years of scientific activities, yet even large trials failed despite being grounded on solid pathophysiological concepts.[26] The 2 substances, pegcetacoplan and avacincaptad pegol, were able to provide significant levels of inhibition of GA lesion growth measured on FAF.[22,27] However, the trial design based on FAF, a late marker of complete RPE loss, did not allow a more in-depth insight into the biological impact of complement inhibition. Moving toward a diagnostic approach such as OCT-based deep learning targeting PR changes offers a wealth of additional information. Inhibition of PR integrity loss seen as EZ loss on OCT is more pronounced than the reduction in RPE loss by pegcetacoplan treatment. Compared with the demarcation on 2D FAF images, which are also compromised by macular pigment shadowing such cellular detection, methods by volumetric OCT imaging should be more sensitive to identify cellular integrity or damage and its defined border. Histology of GA lesion borders reveals a transitional zone of multiple types of cellular alteration including neurosensory degeneration as well as different grades of increasing RPE dysmorphia and choriocapillary rarification.[28] The borders of the GA lesion in histology were best correlated with high-quality OCT B-scans.

For identification of the PR condition, our ensemble-based algorithm annotates the top of the EZ to the outer boundary of the third hyperreflective outer retinal band.[24] Immunohistochemistry characterization of this outer OCT zone identified the hyperreflective mitochondria-rich outer segments of cones and the hyporeflective band of fragments of cone outer segments and cone phagosomes located on top of the RPE.[29] Morphological analysis further demonstrated that PR loss and alteration as indicated by such an EZ loss on OCT reaches outside the GA margin in the majority of cases.[29] Complement factor 3 inhibition is a promising strategy as complement activation by any pathway leads to cleavage of C3 and amplification of the complement response.[2] Complement is activated on PR outer segments in the retina peripheral to atrophic lesions associated with GA.[30] Activation of the classic and alternative pathway in an experimental model of GA contributed to loss of PR function by progressive degeneration of rods and cones.[30] Photoreceptor loss and thinning as represented by our definition of the corresponding EZ band on OCT consistently have been demonstrated using the identical algorithm in multiple populations.[13,20,24,31,32] In FILLY, EZ loss and thinning correlated consistently with pegcetacoplan therapy versus sham.[20] In an observational study, GA growth rates correlated significantly with the EZ loss area, and recent converters had significantly higher EZ/RPE loss ratios at all time points compared with patients in a more advanced disease status.[13] Other groups have applied different algorithm architectures mostly based on a single U-net to identify biomarkers for GA progression on OCT imaging similarly concluding that OCT-based AI analyses may have substantial advantages to FAF and be recommended for use in future clinical trials.[33,34] Most important, 3D layer segmentation on OCT by AI achieved the best metrics on en face heatmaps and B-scan grading tasks, as well as explainable visualizations in the detection of GA as suggested by retina experts.[35]

The third contribution of our analysis focusses on providing prognostic features for disease activity and therapeutic response. Genetic analysis failed as a predictive method as

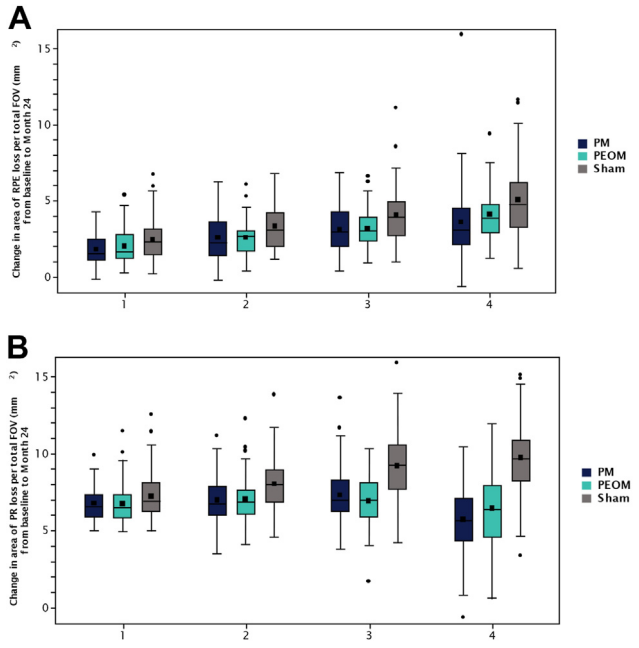

Figure 7. Treatment effect between ellipsoid zone (EZ) loss growth between EZ-retinal pigment epithelium (RPE) loss difference quartiles (1-4) and treatment arms. **A,** The treatment effect on RPE loss growth between quartiles. **B,** The treatment effect on EZ layer maintenance between quartiles. Note that the treatment effect between pegcetacoplan monthly (PM)/pegcetacoplan every other month (PEOM) treatment arms and sham gets more pronounced in higher quartiles and particularly on the EZ layer integrity. FOV = field of view.

genetic subtypes indicated a risk, but not the progression over time.[36] Morphological changes in the macula are obvious prognostic targets. By OCT, local GA progression speed correlated positively with local increase of hyper-reflective foci.[37] Global progression speed did not correlate with hyper-reflective foci concentrations. Subclinical features such as neurosensory layer thinning attract much interest with the ability of quantification by AI-based measurement. Artificial intelligence–based visualization of lesion growth over time at the level of EZ and RPE demonstrates a consistent pattern of faster and wider expansion of lesions with high EZ loss outside RPE loss, that is, a high EZ-RPE difference at baseline. With this biomarker, disease activity is objectively predicted by a morphological parameter that can be visualized at the first visit. In irreversible disease such as GA, this is clinically relevant information because it provides a decision criterion for the physician to evaluate treatment options and for the patient to recognize an imminent risk of vision loss. Most important, the ability to recognize individual disease activity at baseline presentation should allow timely treatment decisions without waiting for more loss of functional retinal tissue. In contrast to an estimation of lesion growth on a population base,[6,8] this approach is highly personalized and indicates in an en face representation the future location of lesion extension (e.g., subfoveal versus nonsubfoveal). Prediction of future GA growth speed was not within the scope of the presented analysis. The novel finding in our work is the impact of the EZ-RPE difference on disease activity compared between the different quartiles of EZ-RPE loss and a similar influence on the therapeutic response to C3 inhibition. However, the results of the relationship between EZ-RPE loss difference quartiles and disease activity and therapeutic response should be interpreted with caution because the number of patients in the groups is small. This is because of a division by the 3 treatment arms and a division by quartiles. Additional studies and longitudinal testing will be needed to further evaluate these findings, yet the signals found for a role of the EZ-RPE loss difference in respect to disease progression and therapeutic response are consistent and have been noted in smaller studies and various analyses by other investigators[20,38–41] but never in such an exemplary therapeutic trial as the phase III trials of DERBY and OAKS.

Availability of the first efficient therapeutic options in GA as one of the most relevant causes for visual disability globally is a promising horizon. However, the burden of disease equals the challenge of diagnostic and therapeutic care by lifelong intravitreal injections in millions of individuals. Moreover, the conventional parameter for determining treatment success, which is improvement in vision, does not easily apply to GA given its progressive, irreversible nature.[42] Although there was a higher treatment effect on the PR condition, the OAKS study could not show any significant treatment-related difference on mean visual sensitivity on microperimetry but a significant effect on the number of scotomatous points at the junctional zone. However, PR thickness does correlate with sensitivity, which is the general state of knowledge to date.[16,43] To date, GA trials have focused on BCVA change, which has never been reached in any phase 3 GA trial, particularly not one with a large proportion of subfoveal lesions. Therefore, additional MP was performed in one of the trials, OAKS. However, the type of lesions in the trial in combination with the fixed grid resulted in the positioning of MP spots in the center of the OCT where most of the RPE loss areas were observed. This resulted in a spatial bias with respect to the lesion and MP spot distribution. Although most areas without EZ and RPE loss are in the periphery of the FOV, most MP spots were already irreversibly damaged, without the possibility of a treatment effect, with only a few points remaining to observe a treatment effect, that is, areas with EZ loss alone. The percentage of more than 26 000 analyzed points from the OAKS study located within EZ loss areas alone (without underlying RPE loss) was approximately 13% at baseline and 10% at month 24. A total of 10% to 13% of "targeted" test points, targeted referring to a location directly on the area of PR alteration cannot be powered to provide evidence of therapy-induced change. Particularly, the variability between the spot number in individual lesions varied highly and was not evenly distributed. Also, large FAF, that is, RPE loss lesions ($\leq$ 17.5 mm^2), were included where the surrounding zone of EZ loss grew far outside of the MP grid. Smaller lesions in the lowest EZ-RPE quartile did not progress and could not show significant changes in the sensitivity around the GA lesion. By using FAF or scanning laser ophthalmoscopy imaging, the zone of EZ loss could not be visualized and MP spots could not be placed directly on the areas of interest, that is, the EZ loss area. Moreover, the EZ loss zone is irregular around each individual lesion which further prevents aiming at this area with a test spot invariably placed around a fixed 250-μm perilesional belt. More

correlation spots were lost because of fixation deficits in patients with subfoveal lesions. All of these aspects contributed to a lack of signal in prespecified MP measurement. With the capacity of today's image analysis visualizing the location and extension of EZ loss accurately, a targeted structure/function analysis can be performed resulting in a systematic functional scanning of the area of interest, that is, EZ loss using a morphology-driven approach.

In the report from the NEI/FDA Endpoints Workshop on Age-Related Macular Degeneration, the panel suggested to accept EZ area loss as a surrogate marker with the notion that although an anatomic end point might be considered clinically significant, the critical factors are the extent and location of the change.[42] In our analysis of OAKS and DERBY, we are able to quantify and localize the therapeutic effect on standard OCT images. The FDA experts also suggested the use of AI-based methods to achieve reliability and precision in the PR measurements, a path that we are following closely. Most important, we can provide clinically relevant guidance for predicting the level of therapeutic benefit based on the individual EZ-RPE difference. This is an important paradigm shift in the controversial discussion of the risk/benefit ratio in GA therapy based on average values by FAF imaging. Preservation of RPE alone is a late effect but can be reinforced by adequate patient selection. Preservation of EZ integrity might be a relevant factor in respect to its role as an anatomic correlate for retinal function and correlate of future GA growth.[15,16] Because the PR condition is not deducible for the human expert using OCT images alone, this evaluation necessarily requires AI-based technology that is now becoming available. There were no safety concerns during the study period of OAKS and DERBY; however, a reliable risk/benefit assessment is mandatory in clinical routine regarding the potential complications of therapeutic intervention such as new-onset retinal exudation.[44] Until now, reports of severe inflammatory reactions or retinal vascular occlusion are sparse, but may and often do occur with any therapeutic intervention and the burden of decision-making is significant for physicians.[45] Artificial intelligence–based tools as suggested by our analyses are substance-independent and can be applied in real-world routine by the cloud and in clinical trials to differentiate fast from slow progressors and monitor the therapeutic efficacy in an objective and precise manner.

Study Limitations

Limitations of our study include the retrospective nature in a post hoc approach that is a consequence of the recent availability of deep learning technology after the initiation of the OAKS and DERBY trials. Also, most lesions were already large at study initiation, with a mean of 8 mm^2, and $>$ 24 months a proportion of lesions have expanded beyond the OCT field available for analyses. OCT volumes that expanded outside the FOV were not excluded in this analysis to avoid any bias. However, we believe that the number of scans outside the FOV balances out between the treatment arms and should not affect the statistical analysis. This aspect applies particularly to the areas of EZ loss that result in a ceiling effect mostly during the second year simulating no further growth. Peripapillary atrophy continuous with the GA lesion on FAF was an exclusionary criterion at baseline. However, confluent peripapillary atrophy at later time points has not been excluded because the exact border to the GA lesion cannot be distinguished. Moreover, we expect that peripapillary atrophy presence and area were randomly distributed throughout the treatment arms and would be unlikely to impact overall findings. The results regarding RPE and EZ lesion growth patterns are obviously descriptive and do not refer to causal relationships. For instance, complement activation is most abundant within the choriocapillary layer and flow voids have been suggested as a cause of PR degeneration.[46] More features will become accessible to quantified AI-based imaging and will contribute to the identification of clinically relevant biomarkers. However, PR-related features such as EZ loss are likely the layer of major interest.[42] Future studies are needed to evaluate the impact of the EZ-RPE difference as a predictor of future GA growth characteristics. Another important consecutive step is to provide a distinct structure/function correlation that relates the specific EZ values to retinal performance. In our analysis, there was a decrease in EZ loss area initially. When evaluating these results, it is important to consider that OCT imaging is not histology, but a light reflectance image and the algorithm therefore segments a reflectivity signal, which can change over time due to a biological change in the ultrastructure of the feature or due to reflectivity changes by the orientation of the OCT scan.[47] It is possible that PR may recover under therapy in their OCT appearance, which is substantiated by the fact that this "improvement" occurred in the treatment groups and not in sham. OCT provides image-based biomarkers, such as DRIL, intraretinal cystoid changes, or in general any layer-related parameter. The FDA approval of EZ layer loss on OCT as a primary outcome marker has been a groundbreaking step toward recognition of image-based biomarkers, accepting that biology and imaging may be consistent categories. A promising manner is a point-to-point registration of OCT morphology and microperimetry test locations. Microperimetry has been performed in OAKS but not in a targeted manner that compromises correlations in subgroups. The analyses focused on Spectralis OCT imaging that represents the majority of images obtained in OAKS and DERBY to keep the data set homogenous but the method is device independent.

Conclusions

Our analyses of a large population from 2 prospective randomized clinical trials phase 3 using OCT-based AI methods were able to identify and quantify PR degeneration, defined as EZ loss, and RPE loss in a plausible and clinically relevant manner. Meaningful and innovative results were obtained to assess individual disease activity and therapeutic maintenance in complement-inhibitory therapy in GA. Robust evidence could be provided on the pathomechanisms of GA progression with PR degeneration seen as EZ loss on OCT driving the progression in GA lesions

and RPE loss following as a consecutive event. With determination of the role of the EZ-RPE loss difference for the first time, an objective parameter defining individual progression during the natural course of disease and under therapy could be defined. The EZ-RPE difference had an impact on disease progression and therapeutic response. The analysis also highlights the full potential of C3 inhibition in a comprehensive manner revealing that reductions in PR degeneration are potentially higher than the effect on RPE loss. Identification of patients with higher EZ-RPE difference may become an important criterion for the management of GA secondary to AMD and allow objective assessment of the risk/benefit ratio of the novel therapy optimizing outcomes on a large scale. Recently, EZ thinning has obtained regulatory approval as a primary outcome measure in the first degenerative macular disease, macular telangiectasia.[17] Artificial intelligence−based clinical tools will become widely available via cloud-based technology, which further facilitates real-time and ubiquitous access to a therapeutic option for one of the most severe diseases in our societies. Our research effort undertaken in this context may add another step for envisioning clinical end points and medical devices that eventually will benefit providers, health care systems, and patients.

Footnotes and Disclosures

Originally received: December 22, 2023.
Final revision: July 29, 2024.
Accepted: August 8, 2024.
Available online: August 14, 2024.Manuscript no. OPHTHA-D-23-02396.

[1] OPTIMA - Laboratory for Ophthalmic Image Analysis, Department of Ophthalmology and Optometry, Medical University of Vienna, Vienna, Austria.

[2] RetInSight, Vienna, Austria.

[3] Apellis Pharmaceuticals, Boston, Massachusetts.

Disclosure(s):

All authors have completed and submitted the ICMJE disclosures form.

The author(s) have made the following disclosure(s):

U.S.-E.: Scientific Consultant − AbbVie, Allergan, Annecon, Apellis, Aviceda, Bayer, Boehringer Ingelheim, Complement Therapeutix, Galamedix, Heidelberg Engineering, Medscape, Novartis, ONL, RetInSight, Roche, Topcon; Contract Research to the Medical University of Vienna − Apellis, Genentech, Kodiak; Support for attending meetings − AbbVie, Apellis

J.M.: Payment or honoraria − Apellis, Thea

G.S.R.: Contract Research − RetInSight; Consultancy − Bayer; Grants − RetInSight (to institution); Payment or honoraria − Apellis, Bayer, Thea

W.-D.V.: Employment − RetInSight

A.S.: Employment − RetInSight

A.S.M.: Employment − Apellis; Stock and stock options − Apellis Pharmaceuticals

E.F.: Employment − Apellis

L.S.: Employment − Apellis; Payment or honoraria − Apellis Pharmaceuticals

H.B.: Contract Research − Apellis, Heidelberg Engineering; Payment or honoraria − Apellis, Bayer, Roche

The university received financial support from Apellis Pharmaceuticals for the analysis.

Presented in part at: the Annual Meeting of the Association of Research in Vision and Ophthalmology, April 23−27, 2023, New Orleans, Louisiana.

HUMAN SUBJECTS: Human subjects were included in this study. Written informed consent was obtained from all patients before any study-related procedure, and both studies adhered to the tenets of the Declaration of Helsinki. This post-hoc analysis was approved by the Ethics Committee of the Medical University of Vienna.

No animal subjects were used in this study.

Author Contributions:

Conception and design: Schmidt-Erfurth, Mai, Reiter, Riedl, Vogl, Sadeghipour, McKeown, Foos, Scheibler, Bogunovic

Data collection: Schmidt-Erfurth, Mai, Reiter, Riedl, Vogl, Sadeghipour, McKeown, Foos, Scheibler, Bogunovic

Analysis and interpretation: Schmidt-Erfurth, Mai, Reiter, Riedl, Vogl, Sadeghipour, McKeown, Foos, Scheibler, Bogunovic

Obtained funding: N/A

Overall responsibility: Schmidt-Erfurth, Mai, Reiter, Riedl, Vogl, Sadeghipour, McKeown, Foos, Scheibler, Bogunovic

Abbreviations and Acronyms:
AI = artificial intelligence; **AMD** = age-related macular degeneration; **BCVA** = best-corrected visual acuity; **C3** = complement factor 3; **EZ** = ellipsoid zone; **FAF** = fundus autofluorescence; **FDA** = Food and Drug Administration; **FOV** = field of view; **GA** = geographic atrophy; **MNV** = macular neovascularization; **PEOM** = pegcetacoplan every other month; **PM** = pegcetacoplan monthly; **PR** = photoreceptor; **RPE** = retinal pigment epithelium.

Keywords:
Age-related macular degeneration, Artificial intelligence, Complement inhibitory treatment, Geographic atrophy, OCT, Pegcetacoplan.

Correspondence:
Ursula Schmidt-Erfurth, MD, Department of Ophthalmology, Medical University of Vienna, Spitalgasse 23, 1090 Vienna, Austria. E-mail: ursula.schmidt-erfurth@meduniwien.ac.at.

References

1. Fritsche LG, Fariss RN, Stambolian D, et al. Age-related macular degeneration: genetics and biology coming together. *Annu Rev Genomics Hum Genet*. 2014;15:151−171.
2. Wykoff CC, Hershberger V, Eichenbaum D, et al. Inhibition of complement factor 3 in geographic atrophy with NGM621: Phase 1 dose-escalation study results. *Am J Ophthalmol*. 2022;235:131−142.
3. Boyer DS, Schmidt-Erfurth U, van Lookeren Campagne M, et al. The pathophysiology of geographic atrophy secondary to age-related macular degeneration and the complement pathway as a therapeutic target. *Retina*. 2017;37(5):819−835.
4. Bakri SJ, Bektas M, Sharp D, et al. Geographic atrophy: mechanism of disease, pathophysiology, and role of the complement system. *J Manag Care Spec Pharm*. 2023;29(5-a Suppl):S2−s11.

5. Vangsted A, Thinggaard BS, Nissen AHK, et al. Prevalence of geographic atrophy in Nordic countries and number of patients potentially eligible for intravitreal complement inhibitor treatment: a systematic review with meta-analyses and forecasting study. *Acta Ophthalmol*. 2023;101(8):857–868.
6. Jaffe GJ, Chakravarthy U, Freund KB, et al. Imaging features associated with progression to geographic atrophy in age-related macular degeneration: classification of atrophy meeting report 5. *Ophthalmol Retina*. 2021;5(9):855–867.
7. von Rückmann A, Fitzke FW, Bird AC. Fundus autofluorescence in age-related macular disease imaged with a laser scanning ophthalmoscope. *Invest Ophthalmol Vis Sci*. 1997;38(2):478–486.
8. Hwang JC, Chan JWK, Chang S, Smith RT. Predictive value of fundus autofluorescence for development of geographic atrophy in age-related macular degeneration. *Invest Ophthalmol Vis Sci*. 2006;47(6):2655–2661.
9. Kaiser PK, Karpecki PM, Regillo CD, et al. Geographic Atrophy Management Consensus (GA-MAC): a Delphi panel study on identification, diagnosis and treatment. *BMJ Open Ophthalmol*. 2023;8(1):e001395.
10. Schmidt-Erfurth U, Klimscha S, Waldstein SM, Bogunović H. A view of the current and future role of optical coherence tomography in the management of age-related macular degeneration. *Eye (Lond)*. 2017;31(1):26–44.
11. Pandya BU, Grinton M, Mandelcorn ED, Felfeli T. Retinal optical coherence tomography imaging biomarkers: a review of the literature. *Retina*. 2024;44(3):369–380.
12. Li M, Dolz-Marco R, Huisingh C, et al. Clinicopathologic correlation of geographic atrophy secondary to age-related macular degeneration. *Retina*. 2019;39(4):802–816.
13. Coulibaly LM, Reiter GS, Fuchs P, et al. Progression dynamics of early versus later stage atrophic lesions in non-neovascular age-related macular degeneration using quantitative OCT biomarker segmentation. *Ophthalmol Retina*. 2023;7(9):762–770.
14. Arslan J, Samarasinghe G, Benke KK, et al. Artificial intelligence algorithms for analysis of geographic atrophy: a review and evaluation. *Transl Vis Sci Technol*. 2020;9(2):57.
15. Sayegh RG, Kiss CG, Simader C, et al. A systematic correlation of morphology and function using spectral domain optical coherence tomography and microperimetry in patients with geographic atrophy. *Br J Ophthalmol*. 2014;98(8):1050–1055.
16. Takahashi A, Ooto S, Yamashiro K, et al. Photoreceptor damage and reduction of retinal sensitivity surrounding geographic atrophy in age-related macular degeneration. *Am J Ophthalmol*. 2016;168:260–268.
17. Sallo FB, Leung I, Clemons TE, et al. Correlation of structural and functional outcome measures in a phase one trial of ciliary neurotrophic factor in type 2 idiopathic macular telangiectasia. *Retina*. 2018;38(Suppl 1):S27–S32.
18. MedPage T. Ocular implant producing neurotrophic factor preserves central vision in MacTel. https://www.medpagetoday.com/meetingcoverage/aao/107231. Published 2023. Accessed April 25, 2024.
19. Stealth B. StealthBio Therapeutics Announces Positive End-of-Phase 2 Meeting with FDA on the Development of Elamipretide in Patients with Dry Age-related Macular Degeneration. Available at: https://www.prnewswire.com/news-releases/stealth-biotherapeutics-announces-positive-end-of-phase-2-meeting-with-fda-on-the-development-of-elamipretide-in-patients-with-dry-age-related-macular-degeneration-301848690.html. Accessed January 3, 2024.
20. Riedl S, Vogl WD, Mai J, et al. The effect of pegcetacoplan treatment on photoreceptor maintenance in geographic atrophy monitored by artificial intelligence-based OCT analysis. *Ophthalmol Retina*. 2022;6(11):1009–1018.
21. Mai J, Lachinov D, Riedl S, et al. Clinical validation for automated geographic atrophy monitoring on OCT under complement inhibitory treatment. *Sci Rep*. 2023;13(1):7028.
22. Heier JS, Lad EM, Holz FG, et al. Pegcetacoplan for the treatment of geographic atrophy secondary to age-related macular degeneration (OAKS and DERBY): two multicentre, randomised, double-masked, sham-controlled, phase 3 trials. *Lancet*. 2023;402(10411):1434–1448.
23. Lachinov D, Seeböck P, Mai J, et al. *Projective Skip-Connections for Segmentation Along a Subset of Dimensions in Retinal*. Cham: Springer International Publishing; 2021:431–441.
24. Orlando JI, Gerendas BS, Riedl S, et al. Automated quantification of photoreceptor alteration in macular disease using optical coherence tomography and deep learning. *Sci Rep*. 2020;10(1):5619.
25. Feuer WJ, Yehoshua Z, Gregori G, et al. Square root transformation of geographic atrophy area measurements to eliminate dependence of growth rates on baseline lesion measurements: a reanalysis of age-related eye disease study report no. 26. *JAMA Ophthalmol*. 2013;131(1):110–111.
26. Edmonds R, Steffen V, Honigberg LA, Chang MC. Alternative complement pathway inhibition by lampalizumab: analysis of data from Chroma and Spectri phase III 3. *Ophthalmol Sci*. 2023;3(3):100286.
27. Khanani AM, Patel SS, Staurenghi G, et al. Efficacy and safety of avacincaptad pegol in patients with geographic atrophy (GATHER2): 12-month results from a randomised, double-masked, phase 3 trial. *Lancet*. 2023;402(10411):1449–1458.
28. Li M, Huisingh C, Messinger J, et al. Histology of geographic atrophy secondary to age-related macular degeneration: a multilayer approach. *Retina*. 2018;38(10):1937–1953.
29. Cuenca N, Ortuño-Lizarán I, Pinilla I. Cellular characterization of OCT and outer retinal bands using specific immunohistochemistry markers and clinical implications. *Ophthalmology*. 2018;125(3):407–422.
30. Katschke Jr KJ, Xi H, Cox C, et al. Classical and alternative complement activation on photoreceptor outer segments drives monocyte-dependent retinal atrophy. *Sci Rep*. 2018;8(1):7348.
31. Rivail A, Vogl WD, Riedl S, et al. Deep survival modeling of longitudinal retinal OCT volumes for predicting the onset of atrophy in patients with intermediate AMD. *Biomed Opt Express*. 2023;14(6):2449–2464.
32. Vogl WD, Riedl S, Mai J, et al. Predicting topographic disease progression and treatment response of pegcetacoplan in geographic atrophy quantified by deep learning. *Ophthalmol Retina*. 2023;7(1):4–13.
33. Zhang G, Fu DJ, Liefers B, et al. Clinically relevant deep learning for detection and quantification of geographic atrophy from optical coherence tomography: a model development and external validation study. *Lancet Digit Health*. 2021;3(10):e665–e675.
34. Kalra G, Cetin H, Whitney J, et al. Machine learning-based automated detection and quantification of geographic atrophy and hypertransmission defects using spectral domain optical coherence tomography. *J Pers Med*. 2022;13(1):37.
35. Elsawy A, Keenan TDL, Chen Q, et al. Deep-GA-Net for accurate and explainable detection of geographic atrophy on OCT scans. *Ophthalmol Sci*. 2023;3(4):100311.
36. den Hollander AI, Mullins RF, Orozco LD, et al. Systems genomics in age-related macular degeneration. *Exp Eye Res*. 2022;225:109248.
37. Schmidt-Erfurth U, Bogunovic H, Grechenig C, et al. Role of deep learning-quantified hyperreflective foci for the prediction

of geographic atrophy progression. *Am J Ophthalmol*. 2020;216:257–270.
38. Reiter GS, Told R, Schranz M, et al. Subretinal drusenoid deposits and photoreceptor loss detecting global and local progression of geographic atrophy by SD-OCT Imaging. *Invest Ophthalmol Vis Sci*. 2020;61(6):11.
39. Pfau M, von der Emde L, de Sisternes L, et al. Progression of photoreceptor degeneration in geographic atrophy secondary to age-related macular degeneration. *JAMA Ophthalmol*. 2020;138(10):1026–1034.
40. Pfau M, Schmitz-Valckenberg S, Ribeiro R, et al. Association of complement C3 inhibitor pegcetacoplan with reduced photoreceptor degeneration beyond areas of geographic atrophy. *Sci Rep*. 2022;12(1):17870.
41. Fu DJ, Glinton S, Lipkova V, et al. Deep-learning automated quantification of longitudinal OCT scans demonstrates reduced RPE loss rate, preservation of intact macular area and predictive value of isolated photoreceptor degeneration in geographic atrophy patients receiving C3 inhibition treatment. *Br J Ophthalmol*. 2024;108(4):536–545.
42. Csaky K, Ferris 3rd F, Chew EY, et al. Report from the NEI/FDA Endpoints Workshop on Age-Related Macular Degeneration and Inherited Retinal Diseases. *Invest Ophthalmol Vis Sci*. 2017;58(9):3456–3463.
43. Pilotto E, Convento E, Guidolin F, et al. Microperimetry features of geographic atrophy identified with en face optical coherence tomography. *JAMA Ophthalmology*. 2016;134(8):873–879.
44. Wykoff CC, Rosenfeld PJ, Waheed NK, et al. Characterizing new-onset exudation in the randomized phase 2 FILLY trial of complement inhibitor pegcetacoplan for geographic atrophy. *Ophthalmology*. 2021;128(9):1325–1336.
45. Borchert GA, Shamsnajafabadi H, Hu ML, et al. The role of inflammation in age-related macular degeneration-therapeutic landscapes in geographic atrophy. *Cells*. 2023;12(16):2092.
46. Zhang Q, Zheng F, Motulsky EH, et al. A novel strategy for quantifying choriocapillaris flow voids using swept-source OCT angiography. *Invest Ophthalmol Vis Sci*. 2018;59(1):203–211.
47. Griffin SM, Jia Y, Johnson AJ, et al. Directional reflectivity of the ellipsoid zone in dry age-related macular degeneration. *Ophthalmic Surg Lasers Imaging Retina*. 2021;52(3):145–152.